Part I: Predicting Performance of Purolite A532E Resins for Remediation of Comingled Contaminants in Groundwater

Sarah A. Saslow[a]*, Tatiana G. Levitskaia[a], Elsa A. Cordova[a], Nancy M. Avalos[a], Daria Boglaienko[a], Yilin Fang[a], Xuehang Song[a], Amanda Lawter[a], Hilary Emerson[a], Jim Szecsody[a], Christian D. Johnson[a], Carolyn I. Pearce[a*], Vicky L. Freedman[a,b], and Rob D. Mackley[a]

[a] Pacific Northwest National Laboratory, 902 Battelle Boulevard, Richland, WA 99354

[b] Present Address: Sealaska, 1200 6th Ave, Suite 800, Seattle, WA 98101

sarah.saslow@pnnl.gov, tatiana.levitskaia@pnnl.gov, elsa.cordova@pnnl.gov, nancy.avalos@pnnl.gov, daria.boglaienko@pnnl.gov, yilin.fang@pnnl.gov, xuehang.song@pnnl.gov, amanda.lawter@pnnl.gov, hilary.emerson@pnnl.gov, jim.szecsody@pnnl.gov, cd.johnson@pnnl.gov, carolyn.pearce@pnnl.gov, Vicky.Freedman@pnnl.gov, rdm@pnnl.gov

*Corresponding Authors: sarah.saslow@pnnl.gov

Abstract

Ion exchange (IX) resins are used in pump-and-treat (P&T) facilities to remove soluble groundwater contaminants. However, natural anions present at concentrations orders of magnitude higher than contaminants can compete for IX sites and impact resin lifecycles. Here, the Hanford Site's 200 West Area P&T facility (Washington State, USA) was selected as a case study because it currently uses two IX resins: Purolite® A532E (A532E) to remove pertechnetate (TcO_4^-) and DOWEX 21K (DOWEX) to remove uranium from groundwater. Nitrate (NO_3^-), sulfate (SO_4^{2-}), chloride (Cl^-), and carbonate (CO_3^{2-}) anions have been identified to potentially compete for A532E and DOWEX IX sites. Hanford-relevant anion groundwater concentrations were used to design a series of laboratory-scale batch experiments to evaluate the impact of competing anions on resin performance and potential kinetic effects. These data are then modeled to obtain Cl^--normalized equilibrium exchange coefficients (K) needed to predict IX resin performance. The work is presented in two parts, with IX performance evaluated for A532E in Part I and DOWEX in Part II. Part I results demonstrate that TcO_4^- uptake is not impacted by NO_3^-, SO_4^{2-}, Cl^-, CO_3^{2-} (as HCO_3^-) and U(VI) carbonate anions, with $K_{TcO4-/Cl-}$ >4000, likely due to the high selectivity of A532E trihexylammonium sites for the large, weakly hydrated TcO_4^- anion. Other anion K values were $K_{NO3-/Cl-}$ = 20, $K_{SO42-/Cl-}$ = 0.2, $K_{HCO3-/Cl-}$ = 0.09, $K_{U/Cl-}$ = 370 – 1000. These K values provide conservative parameters for predicting A532E performance, and demonstrate that, under these test conditions, A532E will remove TcO_4^- from current and future influent streams to meet groundwater treatment objectives.

Key words: pump-and-treat; technetium; uranium; anion exchange; Hanford

Graphical Abstract:

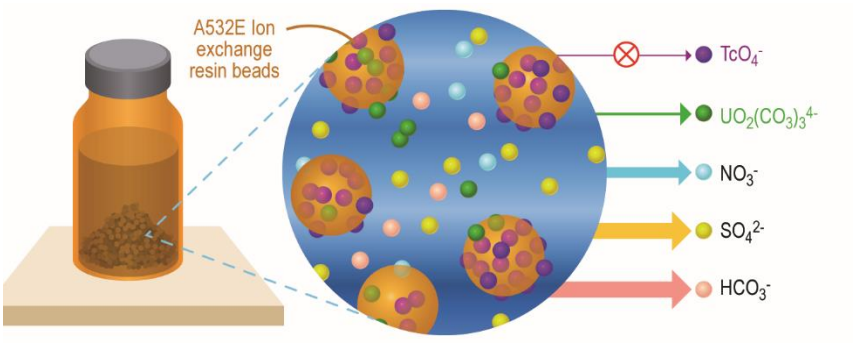

Highlights:

- Targeted batch experiments quantify Purolite® A532E site-specific anion selectivity.
- TcO_4^- uptake by A532E unaffected by groundwater anions NO_3^-, SO_4^{2-}, HCO_3^- and Cl^-.
- U(IV) uptake by A532E does not impact TcO_4^- uptake.
- Derived anion equilibrium exchange coefficients for predicting A532E performance.

1 Introduction

This work aims to reduce the uncertainty associated with the influence of changing groundwater chemistry on ion exchange (IX) resin performance for the removal of radionuclides from contaminated groundwater. Equilibrium IX coefficients (NO_3^-/Cl^-, HCO_3^-/Cl^-, TcO_4^-/Cl^-, and U/Cl^- with U as $UO_2(CO_3)_3^{4-}$) are determined for Purolite A532E (Part I) and DOWEX 21K (Part II) IX resins as a first step to providing a technical basis for future recommendations to optimize groundwater treatment operations, e.g., resin treatment vessel configurations. While this work focused on assessing thermodynamic effects driving IX equilibria with these resins, a preliminary evaluation of IX kinetics was also conducted.

Pump-and-treat (P&T) technology for treating groundwater containing dissolved contaminants (e.g., industrial solvents, metals, radionuclides, and fuel oils) involves pumping groundwater from a network of extractions wells to an above-ground treatment system for contaminant removal prior to re-injection into the subsurface [1]. This approach is commonly used to hydraulically control and/or reduce contaminant concentrations to an acceptable regulatory level [2]. One treatment method by which contaminants are removed from solution in a P&T facility uses IX resins.

A detailed review of the history, development, and different types of IX resins is provided elsewhere [3], and a brief summary is given here. IX is a reversible chemical reaction in which ions in the resin exchange for different ions in solution. IX resins are insoluble polymer beads with an open network structure designed to allow ions to pass through, but the selectivity for specific ions is governed by the nature of IX functional groups. Most commercial IX resins are based on a stable copolymer of styrene and divinylbenzene that is functionalized with exchange sites attached to the copolymer backbone. There are two primary classes of IX resins that specifically target anions: (i) weak base anion resins, functionalized with primary (R-NH2), secondary (R-NHR'), or tertiary (R-NR'2) amine groups that only sorb strong acids with a limited exchange capacity above pH 7.0; and (ii) strong base anion (SBA) exchange resins, functionalized with quaternary ammonium groups (**Figure 1**) that are ionized and can be used over a broad pH range. Two types of quaternary ammonium groups are used in SBA resins: Type I sites have three methyl groups (trimethylamine) and Type II sites have one of the methyl groups replaced with an ethanol group (dimethyl-ethanolamine). Type I resins have greater stability and remove more weakly ionized acids, but are often single-use resins as their regeneration requires strong brine solutions, whereas Type II resins have greater regeneration efficiency. In addition, the internal structure of the resin can vary from gel resins with higher working capacity that do not show porosity in the dry state, to macroporous resins that are two-phase materials with high internal surface area, even in a dry state.

IX resins can be designed to target specific contaminants based on ion properties such as size, charge, and therefore hydration energy. However, targeted contaminant remediation is often complicated by complex and changing groundwater chemistries where abundant natural ionic species compete with the contaminant of concern for available IX sites. Such competing processes have the potential to impact the efficacy of IX resins in a P&T facility. Predicting the behavior of IX resins in the presence of multiple competing ions requires a fundamental understanding of ion

selectivity under the geochemical conditions specific to the groundwater remediation area.

At the U.S. Department of Energy's Hanford Site, a former plutonium production site in southeastern Washington State (USA), groundwater in the Central Plateau (also called the 200 Area) is contaminated with radioactive uranium (U), present as anionic uranyl ($U(VI)O_2^{2+}$) carbonate complexes, and technetium-99 (Tc-99), present as anionic pertechnetate, $Tc(VII)O_4^-$. The 200 West Area (200W) P&T facility is currently using IX resins to treat U and Tc-99. The IX resins are not regenerated when spent and are disposed of on site in the Environmental Restoration Disposal Facility. 200W P&T facility operations rely on two Type I SBA polystyrene-divinylbenzene gel resins to treat groundwater influent: (i) Purolite® A532E (A532E), with bifunctional quaternary amine (triethylammonium and trihexylammonium) functional groups, to remove large, weakly hydrated anions such as TcO_4^- [4-10]; and (ii) DOWEX 21K (DOWEX), with trimethylammonium functional groups, to remove U carbonate species (**Figure 1**) [11]. The 200W P&T system consists of two treatment trains in series with three IX vessels in each train in a lead-lag-polish configuration. The three-vessel configuration is a conservative design that provides the opportunity to operate the lead vessel to exhaustion because the lag and polish vessels capture any contaminant that bleeds through the lead vessel (Figure S1) [12]. In the current configuration, the DOWEX removes U first, then A532E removes Tc-99; however, future operations may change this configuration placing the A532E train first. The incoming water volume and characteristics are different for the two treatment trains, with the U influent tank (Y10) receiving water from a perched water zone, the 200 East Area, and the UP-1 operable unit in 200W, and the Tc-99 influent tank (Y20) receiving water from two additional operable units in 200W (Figures S1 and S2). This study is presented in two parts, A532E performance for the removal of Tc-99 is evaluated here in Part I and the performance of DOWEX for the removal of U will be evaluated in Part II.

Groundwater is extracted from multiple operable units (OUs) and blended in Tank Y20 to form the influent stream to the Tc-99 IX columns (Figure S1 and S2). Table 1 shows the composition of the blended groundwater; Tc-99 concentrations exceed the regulated maximum contaminant level of 900 pCi/L for beta-emitters [13]. The Tc-99 IX treatment train removes Tc-99 from contaminated groundwater to achieve a treated effluent target Tc-99 concentration of 60% (or 540 pCi/L) of the final cleanup level under normal operations [12]. Valenta and colleagues reported Tc-99 partition coefficient (K_d) values of >19,300 mL/g for A532E in deionized water [10]. However, Tc-99 is typically co-located with other groundwater anions, including sulfate (SO_4^{2-}) and nitrate (NO_3^-, Figure S2), with concentrations varying over orders of magnitude (Table 1) [12, 14, 15]. Weakly hydrated NO_3^- is particularly competitive for the IX sites in A532E. Recent characterization of spent Purolite A530E resin (the microporous form of A532E), used for treatment in the 200W P&T facility for 4 years, confirmed that accumulation of NO_3^- and other competing anions accounted for a significant fraction of the total resin anion exchange capacity [5, 11]. Analysis of spent resin from the lead column (Figure S1) showed that Tc-99 accounted for ~ 0.03% of the theoretical total capacity, whereas NO_3^- and SO_4^{2-} accounted for 79% and 6% of the resin capacity, respectively [5]. Over the 4 years that the A530E resin was in use at the 200W P&T facility, concentrations of NO_3^- and SO_4^{2-} in Tank Y20 were approximately 71 and 52 mg/L, respectively, which is approximately 3×10^6 and 5×10^5 times higher than the Tc-99

concentration, based on molar ratios [5]. Despite these conditions, the Tc-99 concentration in the effluent from the lead column remained below 900 pCi/L for 3 years. Once the Tc-99 concentration in the effluent from the lead column exceed 900 pCi/L, the lag and polish columns removed the remaining Tc-99 to <540 pCi/L and the A530E in the lead column was replaced. In their work on uptake of the weakly hydrated, monovalent perchlorate anion (ClO_4^-), which has similar properties with TcO_4^- and is also selectively removed by A530E, Gu et al. (2005) measured a decrease in the K_d value for ClO_4^- in the presence of increasing SO_4^{2-}, with the K_d decreasing from 375,100 mL/g ($[SO_4^{2-}]$ = 9.61 mg/L) to 180,400 mL/g ($[SO_4^{2-}]$ = 961 mg/L) after 24 hours sorption [9]. Although Gu et al. (2005) did not test TcO_4^-, it is expected to show similar behavior to ClO_4^-, suggesting that the presence of SO_4^{2-} may decrease TcO_4^- uptake by A532E resin.

A532E may also have exchange capacity for U(VI) carbonate complexes based on the A530E work by Gu and others, where A530E sorption affinity and capacity for removing stable $UO_2(CO_3)_2^{2-}$ and $UO_2(CO_3)_3^{4-}$ in simulated groundwater with variable SO_4^{2-} concentration (9.61 to 961 mg/L) was evaluated [9]. Under the conditions used in the Gu et al. study, A350E removed U(VI) efficiently, with high partitioning coefficients (up to 600,000 mL/g) and > 99% sorption, even in the presence of competing SO_4^{2-} anions. Analysis of the spent resin from the 200W P&T facility also revealed that U was taken up by A530E and present at concentrations approximately half that of Tc-99 [5]. Thus, any U(VI) that bleeds through the DOWEX vessels could be removed downstream by A532E, and potentially compete with TcO_4^- for IX sites (Figure S1). This consideration is even more important if the A532E train is placed in front of the DOWEX train in future facility operations. As such, this study evaluates the influence of competitive effects of U and CO_3^{2-} (present as HCO_3^-) on TcO_4^- uptake by A532E resins.

1.1 Influence of changing groundwater chemistry on IX resin performance

The extent to which groundwater and co-contaminant anions compete with Tc-99 for IX sites on A532E depends on the chemical composition of the influent stream to the 200W P&T facility, which varies with the location of the extraction wells across the Hanford Site (Figure S2). Anion concentrations in the influent to the Tc-99 IX columns (Tank Y20) can vary significantly over a 12-month period (Table 1). Changes in P&T influent groundwater, such as increases in competing natural anions and/or co-mingled contaminants, may result in increased competition for IX sites on A532E and decrease Tc-99 removal performance. There are limited published data describing the partitioning of these potentially competing groundwater anions and co-contaminants between the resin and the aqueous phase under conditions relevant to current and future groundwater remediation at the 200W P&T facility. Here, a series of binary and multicomponent batch experiments were conducted to determine the selectivity of A532E for different ions [e.g., TcO_4^-, U(VI) carbonate species, SO_4^{2-}, NO_3^-, Cl^-, and HCO_3^-] and the potential competitive effects that these species have on TcO_4^- removal by A532E. The batch experiments were not designed to replicate the composition of the groundwater influent, but instead to probe the effect of individual anions over a range of concentrations that represent current and future groundwater influent compositions to the 200W P&T facility. These results can then be used as a training set to generate a thermodynamic model for predicting A532E resin performance as a function of changes in influent composition. In IX models, the ion removal mechanism is often considered as a simple

electrostatic interaction. However, this work considers other factors that can significantly impact the thermodynamics and kinetics of IX reactions, including (i) the hydration energy of the exchangeable ions; (ii) the size and nature of counterions; (iii) the types of functional groups on the resin; and (iv) the occurrence of competing sorption reactions [9]. The equilibrium exchange coefficient (K) values (reported for ion pairs NO_3^-/Cl^-, HCO_3^-/Cl^-, TcO_4^-/Cl^-, and $UO_2(CO_3)_3^{4-}/Cl^-$) calculated from these batch sorption data will be used generate a thermodynamic model for predicting A532E performance. As kinetic effects can play an important role in Tc-99 uptake efficiency under the dynamic conditions in the IX vessels at the 200W P&T facility, a future study will evaluate IX performance under flow conditions. Column experiments will be conducted, firstly with a synthetic groundwater containing the anions included in the batch experiments performed here, and then secondly with actual groundwater from the 200 Area, with the batch-derived K values used in flow and transport modeling to fit Tc-99 breakthrough data. The model will be optimized to account for both thermodynamic and kinetic effects, then ultimately scaled up to provide operational feedback to the 200W P&T facility, and to inform future resin treatment train design for optimization of both U and Tc-99 removal.

2 Materials and Methods

2.1 Materials.

The Purolite® A532E resin (A532E) is a Type I SBA with a gel polystyrene polymer structure crosslinked with divinylbenzene and functionalized with quaternary ammonium sites (tri-n-hexylamine/tri-n-ethylamine). The A532E resin has the appearance of spherical beads (0.650 ± 0.050 mm in diameter) and in the Cl^- form has a reported total capacity of ≥0.6 eq/L by the manufacturer [4]. Prior to use in batch experiments, A532E resin beads were pre-conditioned with 1 M NaCl to maximize loading capacity. Resin stripping experiments were used to measure the actual total exchange capacity for the pre-conditioned resins, and results show that the total exchange capacity for Cl^- loaded A532E resin is 1.12 meq/g dry resin. When normalized to the mass of wet resin, the total exchange capacity, 0.48 meq/g wet resin, is similar to the manufacturer reported value. The pre-conditioned A532E resin was also used to measure the average resin moisture content, which ranged from 54 – 60 wt% depending on the batch of pre-conditioned A532E resin used for a specific experiment. Experimental details for resin pre-conditioning, stripping, and moisture content measurements are provided in the supporting information (SI).

2.2 Solution Preparation for Batch Experiments.

All anions (except for Tc-99 and U) were added as a sodium salt in double deionized water (DDI), e.g., Cl^- as NaCl, CO_3^{2-} as Na_2CO_3, NO_3^- as $NaNO_3$, and SO_4^{2-} as Na_2SO_4 (Table 2). Uranyl chloride trihydrate ($UO_2Cl_2 \cdot 3H_2O$, International Bio-Analytical Industries) and ammonium pertechnetate (NH_4TcO_4, synthesized in house) were used to prepare 11.6 and 20 mg/L stock solutions, respectively, in DDI. The experiment matrix and target concentrations for Cl^-, CO_3^{2-}, NO_3^-, SO_4^{2-}, Tc-99, and U used for each batch sorption experiment are provided in

Table 2. A range of solution-to-solid ratios was selected so that the resin would be at 10% – 90% in the form of the contaminant of interest, and the change in solutions concentrations would be larger than the uncertainty in the analysis; a single stock solution was used for these experiments (Tests A, B, D, E, I, K, and Q). For the remaining experiments with variable concentrations of Cl^- (Tests C and J), NO_3^- (Tests F – H and S), and SO_4^{2-} (L – N and R), solutions of 2 M Cl^-, 2 M NO_3^-, and 1 M SO_4^{2-} were made in DDI and spiked into individual experiments to achieve the target concentrations. The target concentrations NO_3^- and SO_4^{2-} were chosen to span the range of concentrations expected for these analytes in Tank Y20, with the range of Cl^- concentrations chosen to represent the total dissolved solids expected [12]. For U and Tc-99 experiments, a 2-mL spike of 20 mg/L Tc-99 and/or a 2-mL 11.6 mg/L U stock solution were added to individual experiments to reach the target Tc-99 and/or U concentrations of 200 and 116 µg/L, respectively. The U and Tc-99 concentrations used here are up to two orders of magnitude greater than the average concentrations expected to be present in the new influent streams from the 200 East Area to allow for better analytical detection of competing anion/contaminant effects on A532E uptake. Prior to addition of the conditioned A532E, the pH was adjusted to 7.4 +/- 0.1 (selected based on the pH of the influent stream to the 200W P&T facility) using diluted HCl or NaOH following the addition all chemicals, and then allowed to equilibrate overnight. On the day of testing, the pH was further adjusted (if needed) and conditioned A532E was added immediately.

2.3 Batch Sorption and Kinetics Experiments.

All batch sorption experiments are outlined in Table 2, were performed in duplicate, and conducted in 250-mL high-density polyethylene (HDPE) bottles. The solution volume was maintained at 200 mL and the mass of A532E was adjusted for experiments that assessed NO_3^-, SO_4^{2-}, CO_3^{2-} (speciation in solution HCO_3^-), TcO_4^-, and/or U(VI) uptake as a function of solution-to-solid ratio (e.g., 50 mL/g used 4 g of dry resin, 100 mL/g used 2 g of dry resin, etc.). The amount of conditioned A532E added to reach the target solution-to-solid ratio was determined according to the dry resin weight, with the actual mass added dependent on the moisture content. Immediately following resin addition, the pH was measured, and the bottles were placed on a shaker at 125 rpm for 72 hours to account for kinetic effects and ensure that the IX reaction reached equilibrium, as demonstrated in the kinetics experiments. The combination of two differently sized trialkylammonium groups in A532E provides a balance between selectivity for sorption of large, poorly hydrated anions, e.g., TcO_4^- (trihexylammonium groups), and faster kinetics facilitated by the more hydrophilic triethylammonium group (**Figure 1**) [16, 17]. At the end of 72 hours, bottles were removed from the shaker and left undisturbed for 5 – 15 minutes to allow the resins to settle out of solution. The final solution pH in each bottle was measured and then two 5-mL aliquots were filtered using a 0.45-µm syringe filter and used for Tc-99 and U quantification by inductively coupled plasma mass spectrometry (ICP-MS) and for anions by ion chromatography (IC). Carbonate uptake was calculated as the milliequivalent difference in Cl^- released, as measured by IC, also accounting for other measured anions removed from solution of known charge. The carbonate uptake from experiments containing U(VI) complexes could not be calculated because the exact charge of the UO_2^{2+} species could not be absolutely determined. Aliquots for ICP-MS analysis were acidified with 2% HNO_3 to stabilize the metals in solution. The reported ICP-MS method limits of detection for Tc-99

ranged from 0.037 to 0.74 µg/L, and for U from 0.152 to 1.52 µg/L. IC method detection limits for Cl (0.067 – 6.7 mg/L), NO_3^- (0.066 - 23 mg/L), and SO_4^{2-} (0.108 - 50.5 mg/L) ranged according to the dilutions required to analyze the samples.

The details above apply to both batch sorption and kinetics testing; however, there are several differences for the kinetics experiments. First, 2-mL aliquots (rather than 5 mL to ensure that the solution volume was maintained within 10%) for U and Tc-99 analysis were collected from the same bottle at 0, 0.50, 1, 2, 4, 8, 24, 48, and 72 hours. Measurements of pH were collected at the same time points following the aliquot collection. Lastly, no aliquot was collected for IC for the kinetic experiments.

The experimental precision of these batch experiments is estimated to be +/-5% and is based on a combination of replicate determinations, volumetric error, and analytical measurement variance. The primary source of error occurs during sample preparation and is reflected in the average solution:solid ratio (mL/g) and standard deviation determined from all A532E experiments with a target solution:solid ratio of 200 mL/g (98 data points), which is 201 ± 11 mL/g of dry resin.

Adsorption Isotherm Models. The ICP-MS and IC results were used to construct sorption isotherms that were fit using a Freundlich adsorption model, as it describes sorption systems possessing dissimilar binding sites. The Freundlich adsorption model is shown in Equation 1 [18]:

$$q_e = K_f C_e^n \qquad \text{Equation 1}$$

where q_e is the anion equilibrium sorption capacity (in meq/g), C_e is the equilibrium anion concentration (in mM), and K_f and n are the adsorbate and resin fitting constants.

2.4 Geochemical Modeling Software

Two geochemical codes were used to simulate solution speciation and resin behavior.

Speciation of anions in solution present at thermodynamic equilibrium was simulated with Geochemists Workbench (GWB 12.0.7, www.gb.com) [19], generating speciation plots. Calculations were performed using the thermodynamic database file thermo.com.V8.R6+.dat that is supplied with GWB, but augmented with selected data from the Organization for Economic Co-operation and Development/Nuclear Energy Agency-Thermochemical Database Project [20-22]. All models were built for temperature of 25 °C and pressure of 1 atm, at the equilibrium with 0.04% (vol.) (or 400 ppm) of CO_2 and 21% (vol.) of O_2 in the atmosphere.

HYDROGEOCHEM is a mechanistic-based numerical model for subsurface coupled fluid-flow and multicomponent reactive transport that was used to calculate anion equilibrium exchange coefficients (K) [23]. The reactive chemistry in HYDROGEOCHEM is solved using BIOGEOCHEM [24, 25], which implements a new paradigm of reaction-based approaches to simulate biogeochemical processes with mixed equilibrium and kinetic reactions. BIOGEOCHEM was used to model the batch IX experiments, using the Gaines-Thomas convention, which uses an equivalent fraction for activity of the exchangeable ions. To determine anion K values, an ensemble of simulations was run given a range of K based on a

one-site model for anion pairs in the following order for A532E: NO_3^-/Cl^- (or SO_4^{2-}/Cl^-), HCO_3^-/Cl^-, TcO_4^-/Cl^-, then $UO_2(CO_3)_3^{4-}/Cl^-$, once the K for each of the other ion pairs were independently determined.

For the following IX reaction between Cl^- and SO_4^{2-}:

$$(Cl - X) + ½SO_4^{2-} \leftrightarrow Cl^- + ½(SO_4 - X_2)$$

the equilibrium exchange coefficient, K, is calculated as defined in Equation 2 [19, 23].

$$K_{SO4/Cl} = \frac{\{SO_4 - X_2\}\{Cl^-\}}{\{Cl - X\}\{SO_4{}^{2-}\}^{0.5}} \quad \text{Equation 2}$$

where $K_{SO4/Cl}$ is the equilibrium coefficient for SO_4^{2-} exchanging parent Cl^- sites on the resin, X is the total number of positively charged exchange sites [where SO_4^{2-} requires two exchange sites per anion (X_2) and the model does not differentiate between two different IX sites], and the brackets { } represent activities calculated within the HYDROGEOCHEM model as a function of anion concentrations.

The K value that minimized the root mean square error (RMSE) of the model fit to the range of experimental data evaluated is reported. The RMSE is calculated as follows:

$$RMSE = \sqrt{\sum \frac{([C_e]_M - [C_e]_E)^2}{n}} \quad \text{Equation 3}$$

Where $[C_e]_M$ is the model predicted concentration (in mM, or µM for Tc-99 and U) of an anion in solution after the batch contact experiments, $[C_e]_E$ is the experimentally determined anion solution concentration after the batch contact experiment, and n is the number of datapoints used to calculate K. Note, that the RMSEs reported are not an indication of goodness of fit and for different anions should not be compared as the number of data points and datapoints representing measurable concentrations (those that fall above instrument limits of detection) are often different.

3 Results and Discussion

3.1 Solution speciation modeling

The anion nature and hydration energy, which is a function of its size and charge, have a significant impact on the thermodynamics and kinetics of IX reactions [16]. Thus, the solution speciation of NO_3^-, SO_4^{2-}, CO_3^{2-}, Tc-99, and U under the experiment conditions was established prior to evaluating uptake by A532E in batch sorption experiments. Anion speciation was modeled with GWB as a function of pH or concentration of major anion of interest, i.e., NO_3^- or SO_4^{2-}, under the aqueous conditions of Test G for the NO_3^- system and Test N for the SO_4^{2-} system. The Tc-99 present in Test H did not impact other anions' speciation. Tc-99 was present as TcO_4^- under all conditions tested. Figure S3 in the SI shows that no speciation changes occurred for CO_3^{2-}, UO_2^{2+}, NO_3^-, and TcO_4^-. Carbonate speciation diagrams (Figure S3A and D) indicate that, under the circumneutral pH experiment conditions, bicarbonate (HCO_3^-) is the dominant anionic species in the solution. UO_2^{2+} was predominantly present as uranyl tricarbonate ($UO_2(CO_3)_3^{4-}$) above ~pH 6.3 irrespective of NO_3^- or SO_4^{2-} concentration. The pH dropped below 6.3 in Tests B and I, but CO_3^{2-} and U were not added to solutions in these experiments. Based on speciation modeling, U loading on resin calculated and reported in Tables S2 and S3 assume a quadrivalent charge for $UO_2(CO_3)_3^{4-}$ and a monovalent charge for HCO_3^-. All anions, except for Tc-99 and U, were added with sodium (Na^+) as the cation, which does not change the speciation of $UO_2(CO_3)_3^{4-}$ under these experimental conditions.

3.2 Binary sorption isotherms

Sorption isotherms for HCO_3^-, NO_3^-, and SO_4^{2-} are presented as fractional loading (q_e in meq/g dry resin) normalized to total resin exchange capacity (q_t), vs. equilibrium analyte concentration (C_e) to compare the affinity of the A532E resins for these anions (Figure 2). The q_t for Cl^- on A532E was determined to be 1.12 meq/g dry resin using the resin stripping procedure detailed in the SI, but in batch sorption experiments, NO_3^- loadings of up to 1.70 meq/g dry resin were obtained (Table S2, Test B). The fractional loadings (q_e) in the batch sorption experiments are calculated from the concentration of ions removed from solution, whereas the q_t for Cl^- is calculated from the concentration of ions remaining on the resin after loading and rinsing, thus, the q_e is likely to be higher. The q_e determined in the batch sorption experiments is the result of equilibration between the solution and the solid phase, and is more influenced by solution feedback resulting in higher values for anions that become more tightly bound to the IX sites due to their size, charge and/or hydration state, e.g. NO_3^- and TcO_4^-. As previously reported for microporous A530E, the lipophilic trihexylammonium sites on these resins preferentially remove more weakly and moderately hydrated anions. Since NO_3^- has a Gibbs free energy of hydration (ΔG_{hyd}) of -306 kJ/mol, it has a greater affinity for the trihexylammonium sites than Cl^- (ΔG_{hyd} =-347 kJ/mol) resulting in a higher q_e than the q_t value determined using the resin stripping procedure [5]. Therefore, the highest experimentally determined q_e value (1.70 meq/g dry resin from the results of Test B) was used as q_t to calculate equilibrium exchange coefficients with the HYDROGEOCHEM numerical-modeling approach discussed in later sections.

A532E also removed SO_4^{2-} from solution in the absence of additional Cl^- (Figure 2D, Test I), but

the highest q_e (1.56 meq/g dry resin) was less than that for NO_3^- (1.70 meq/g dry resin) (Figure 2C). The removal of SO_4^{2-} from solution by A532E was suppressed in the presence of Cl^- because SO_4^{2-} has a much greater hydration energy (ΔG_{hyd} =-1090 kJ/mol), therefore the hydrophobic long-chain alkyl groups in A532E preferentially remove anions in the order NO_3^- > Cl^- > SO_4^{2-} [16].

A Freundlich adsorption model, describing sorption systems with dissimilar binding sites, gave the best fit to the HCO_3^-, NO_3^-, and SO_4^{2-} isotherms for A532E (Figure 2B and D) [18]. Linear fits of the experiment data were obtained for HCO_3^- and NO_3^- at low- to mid-range resin loadings, but the data deviate from the linear trend above ~70% loading of the resin. These results are consistent with previous observations for A530E, the macroporous analog of the gel A532E, whose sorption behavior could also be described by a Freundlich isotherm model [5].

Given the high exchange capacity of A532E, it was necessary to determine a target concentration of Cl^- to use as a background electrolyte in Tests D – H and Tests K – S, such that changes in uptake of the bulk groundwater anions of interest, NO_3^- and SO_4^{2-}, would be measurable. Chloride was chosen as a background electrolyte because it is a common groundwater anion and will compete with NO_3^- and SO_4^{2-} for anion exchange sites at sufficient concentrations. The uptake of NO_3^- (Test C) and SO_4^{2-} (Test J) as a function of background Cl^- concentration was therefore evaluated to identify a target Cl^- concentration where NO_3^- and SO_4^{2-} uptake fell within the desired range of 20% – 80% (Table 2). Sorption of both NO_3^- and SO_4^{2-} was suppressed upon addition of Cl^-, with a corresponding decrease in effective loading (Figure 3). However, the effective loading of SO_4^{2-} decreased more than that of NO_3^-, e.g., at high Cl^- concentrations (200 mM), the loading of NO_3^- on A532E remained relatively high (~ 20%), while SO_4^{2-} loading was < 5%.

Based on the Cl^--dependent NO_3^- sorption isotherm (Figure 3), a 50-mM (1768-mg/L) Cl^- concentration was chosen as the target background electrolyte concentration to achieve NO_3^- uptake of 57% (Table S1). This Cl^- concentration was chosen as a background electrolyte to give optimum NO_3^- uptake, not to represent groundwater concentrations, but it does correspond to the highest total dissolved solids concentration (1873 mg/L) in the 200W P&T remediation area, which was measured in a perched water zone [12]. For consistency, 50 mM Cl^- was used as the background electrolyte concentration for all NO_3^- and SO_4^{2-} experiments, even though SO_4^{2-} uptake at 50 mM Cl^- was only 11% (Table S2).

Test D for NO_3^- and Test Q for SO_4^{2-} were used to determine the NO_3^- and SO_4^{2-} sorption isotherms for A532E in the presence of the target Cl^- concentration (50 mM) as a function of solution-to-solid ratios ranging from 50 – 1000 mL/g dry resin (Figure 2D). For NO_3^-, uptake was 25% – 89% and q_e was 0.14 – 0.77 meq/g. For SO_4^{2-}, uptake was 1% – 35% and q_e was 0.07 – 0.14 meq/g. The Freundlich adsorption model adequately described the IX behavior for NO_3^- (Figure 2D), but the limited uptake of SO_4^{2-} resulted in a poor fit to the data.

3.3 Multicomponent sorption isotherms

The uptake of NO_3^-, SO_4^{2-}, Tc-99, and/or U by Purolite A532E resin was evaluated in the presence of Cl^- (50 mM) using a series of sorption isotherms, each systematically building in

complexity to identify competition among the anions for uptake. The sorption isotherms are shown for NO_3^- (Figure 4) and SO_4^{2-} (Figure 5). The change in pH relative to a blank solution without resin, contaminant loadings (q_e), equilibrium anion aqueous concentration (C_e), and percent uptake are summarized in the SI (Tables S1 and S2).

Multicomponent experiments containing NO_3^-. In Test E, NO_3^- uptake was evaluated after adding carbonate (10 mM) to the background electrolyte (50 mM Cl^-). A small but systematic decrease in NO_3^- loading was observed (Figure 4A) when comparing Test E to Test D (no HCO_3^-), with NO_3^- q_e values decreasing by up to 0.08 meq/g. The NO_3^- sorption isotherm for Test F with Cl^- (50 mM) and TcO_4^- (2 µM) overlaps with the isotherm for Test D without TcO_4^-, suggesting that NO_3^- uptake is the same with or without micromolar concentrations of Tc-99 (Figure 4A). The NO_3^- isotherm for Test H in the presence of all anions of interest, Cl^- (50 mM), carbonate (10 mM), TcO_4^-, (2 µM), and U (0.5 µM), was nearly identical to the NO_3^- uptake for the solution matrix of Cl^- (50 mM) and HCO_3^- (10 mM) in Test E, and in the presence of TcO_4^- (Test S) and U (Test G). These results highlight the high selectivity of A532E for NO_3^-.

Under these experiment conditions, Tc-99 is present as TcO_4^- in solution and on the resin, as predicted by GWB modeling and confirmed by previous characterization of Tc-loaded A530E [5]. Uptake of Tc-99 was > 99% in all experiments (Tests F, H, L, N, R, and S) regardless of the presence of other potentially competing anions. This high selectivity of A532E (and A530E) for Tc-99 in the presence of competing ions has been reported previously [5, 26], and is due to the trihexylammonium exchange sites that are specifically designed to uptake the hydrophobic – weakly hydrated – TcO_4^- anion. The uptake of TcO_4^- by A532E was quantitative regardless of initial Cl^- concentration or NO_3^- concentration, which varied from 0 to ~ 20.3 mM. However, at the highest NO_3^- concentrations in Test F (10 mM and 20 mM), there was a slight increase in the equilibrium aqueous Tc-99 concentration (Figure 4B). This suggests that, when the NO_3^- loading is close to the total exchange capacity for A532E (1.1 – 1.7 meq/g) and the triethylammonium IX sites in the resin are occupied, NO_3^- starts to compete with TcO_4^- for the trihexylammonium IX sites that target poorly hydrated anions. This slight increase in TcO_4^- C_e values at high NO_3^- concentrations was mitigated when 10 mM CO_3^{2-} was added to the system (in the absence of U), highlighting the importance of evaluating competitive effects (Test S). In Test H, with all anions of interest present, Cl^- (50 mM), carbonate (10 mM), TcO_4^-, (2 µM), and U (0.5 µM), TcO_4^- uptake remained > 99%; however, a small but reproducible increase in the equilibrium solution TcO_4^- concentration was observed (Figure 4B), suggesting that U has a slight impact on TcO_4^- uptake. As in Test F, the equilibrium solution concentration of TcO_4^- plateaued at low NO_3^- loading on the resin and started to increase when NO_3^- loading reached ≥ 1.07 meq/g, suggesting that HCO_3^- and U do not compete for the trihexylammonium binding sites occupied by TcO_4^- and NO_3^- at high loading.

U(VI) is present as the uranyl cation (UO_2^{2+}), which coordinates with carbonate to form negatively charged $UO_2(CO_3)_3^{4-}$ complexes, the dominant species under these experiment conditions (Figure S3). Thus, uptake of HCO_3^- by A532E could increase the resins' affinity for U, but the high selectivity of A532E for NO_3^- may counteract this effect. When U (0.5 µM) was introduced in Test G, the NO_3^- isotherm was not significantly affected (Figure 4) and

NO_3^- loading (0.37 meq/g) was about equal to that for Test E with the same experiment conditions in the absence of U (0.38 meq/g). However, U uptake decreased from 92% in the absence of NO_3^- to 67% at the highest initial NO_3^- concentration (20 mM, 2010 ppm, Table S2). The addition of TcO_4^- (Test H) further decreased the uptake of U in the presence of NO_3^-, and increase in NO_3^- concentration from 0 to 19 mM (1160 ppm) resulted in a decrease of U uptake from 92% to ~ 38%. The highly charged $UO_2(CO_3)_3^{4-}$ complex requires four available IX sites (presumably triethyl) on the resin and is outcompeted by high concentrations of monovalent NO_3^-, which requires only one available site for IX. In addition, the increased NO_3^- loading on the resin decreases the IX sites that are occupied by HCO_3^-, resulting in an unfavorable coordination environment for UO_2^{2+} carbonate complexes. With NO_3^- occupying the IX sites, the uptake of U becomes less energetically favorable as the binding energies for the $UO_2(CO_3)_n^{(2n-2)-}$ complexes are more negative (in Kcal/mol) than for the $UO_2(NO_3)_n^{(n-2)-}$ complexes [27]. It should be noted that NO_3^- is a weak ligand and does not coordinate with UO_2^{2+} as evident from the thermodynamic GWB modeling (Figure S3B). This explains the decreasing trend in U uptake with increasing NO_3^- concentration, as NO_3^- replaces HCO_3^- on the IX sites in A532E. The additional decrease in the uptake of U in the presence of Tc-99 (Test H) suggests that there is the potential for competition between these two contaminants for available IX sites when there are significant concentrations of other anions present in solution. However, given that the range of NO_3^- concentrations tested here (0 – 1450 mg/L) is too high to be expected in subsurface contaminated plumes in general and exceeds the likely maximum NO_3^- concentration that will be present in the blended influent stream to the 200W P&T facility, the risk of reaching competitive NO_3^- concentrations during P&T operations is low.

The binary equilibrium exchange coefficients (K) for A532E, calculated from the independent experiments using HYDROGEOCHEM, were determined to be $K_{NO3-/Cl-}$, $K_{HCO3-/Cl-}$, and $K_{TcO4-/Cl-}$ in Test H as 20, 0.09, and >4000, respectively. These K values indicate where agreement between model predicted anion C_e values and experimentally measured anion C_e values produced the lowest RMSE value. These coefficients were then fixed to estimate $K_{U/Cl-}$ assuming $UO_2(CO_3)_3^{4-}$ as the exchanged anion. The best estimate of $K_{U/Cl-}$ using combined data from Test G and Test H is 500 and suggests that Tc-99 will out-compete U for uptake 8:1 ($K_{TcO4-/Cl-}$/ $K_{U/Cl-}$) when both contaminants are present with high concentrations of other anions. The comparison between the observations and the simulated results is shown in Figure 6 (Test G and Test H).

Multicomponent experiments containing SO_4^{2-}. The batch sorption experiments conducted with SO_4^{2-} are summarized in Figure 5 and Table S3. Tests K and Q were conducted to quantify SO_4^{2-} uptake in presence of HCO_3^- and Cl^-, and Cl^- only, respectively. A slight decrease (0.01 – 0.07 meq/g) in the SO_4^{2-} equilibrium sorption capacity occurred when HCO_3^- was present in addition to Cl^-. In the presence of TcO_4^-, Cl^- and HCO_3^- (Test R) and U (Test N), the SO_4^{2-} equilibrium sorption capacity (0 – 0.29 meq/g) was the same +/- 0.01 meq/g. However, the SO_4^{2-} equilibrium sorption was higher with only Tc and Cl^- present (Test L), highlighting that HCO_3^- outcompetes SO_4^{2-} for IX sites on A532E. The results in Test M, with U, HCO_3^-, and Cl^-, were similar to the results from Test L up to 2 mM SO_4^{2-} C_e, then plateaued at approximately q_e = 0.29 meq/g compared to 0.44 meq/g at the highest SO_4^{2-} concentration in Test L.

As with the NO_3^- multicomponent experiments, TcO_4^- uptake in the SO_4^{2-} experiments was still >

99% even at SO_4^{2-} concentrations up to 10 mM. This is in contrast to experiments performed by Gu et al. that found ClO_4^- uptake by similar resin A530E decreased in the presence of elevated SO_4^{2-} concentrations, and suggests that a direct inference of TcO_4^- behavior and A532E resin performance based on ClO_4^- and A530E results may not always be appropriate [9]. The apparent drop in TcO_4^- C_e for Test L (Figure 5B) is due to a difference in ICP-MS detection limit (0.074 ppb for Test L compared to 0.37 ppb for Tests N and R). At the highest SO_4^{2-} concentration (10 mM), U uptake decreased from 96% to 88% (Table S3), both in the presence (Test N) and absence (Test M) of Tc-99 (Figure 5D), suggesting that U uptake may continue to decrease at SO_4^{2-} concentrations exceeding 10 mM.

The binary equilibrium exchange coefficients (K) for A532E, calculated from the independent experiments using HYDROGEOCHEM, were used to determine $K_{SO42-/Cl-}$, $K_{HCO3-/Cl-}$, and $K_{TcO4-/Cl-}$ in Tests M and N as 0.2, 0.09, and >4000, respectively. These coefficients were again fixed to estimate $K_{U/Cl-}$ assuming $UO_2(CO_3)_3^{4-}$ as the exchanged anion. The best estimate of $K_{U/Cl-}$ for Test M was 370, but increased to 1,000 in Test N, which suggests that Tc-99 will still out-compete U for uptake 4:1 ($K_{TcO4-/Cl-}$/ $K_{U/Cl-}$) when both contaminants are present with high concentrations of other anions.

3.4 Batch Sorption Kinetics

Kinetic experiments were conducted to confirm that the IX reaction had reached equilibrium over the time of the batch sorption experiments, and to determine the rate of contaminant uptake so that operating conditions for future column experiments could be optimized. Batch sorption experiments were conducted to determine the kinetics of Tc and U uptake by A532E from a solution containing NO_3^- (19 mM), SO_4^{2-} (5 mM), Cl^- (50 mM), and CO_3^- (10 mM) (Test T, Table 2) over 72 hours. Results suggest that the zero-order model provides the best fit for Tc-99 (R^2 = 0.812) uptake by A532E (Figure S4). Most of the Tc-99 was removed during the first 8 hours, and equilibrium was reached after 24 hours. The rate constant (K) for zero-order reaction kinetics of removal of Tc-99 over the initial 8-hour period was calculated to be 26 µg/(g hr) (Figure S4B). The extent of Tc-99 uptake (> 99 %) after 72 hours in these kinetic experiments was comparable to that for Tc-99 uptake in the presence of NO_3^- only (Test H, 0 – 19 mM) and SO_4^{2-} only (Test N, 0 – 10 mM). The uptake of U in the presence of increasing NO_3^- concentrations ranged from 92% – 38% (Test H), and the uptake of U in the presence of increasing SO_4^{2-} concentrations ranged from 96% – 88% (Test N). Thus, when high concentrations of both NO_3^- and SO_4^{2-} are present in solution, as in Test T, the uptake of U is minimal, making it difficult to determine a rate order and constant.

4 Conclusions

The 200W P&T facility at the Hanford Site uses Purolite A532E resin in the IX system as it is specifically designed to target TcO_4^- removal from the groundwater influent. This work assessed the impact of a broader range of influent chemistries on A532E resin performance to confirm that A532E will continue to remove TcO_4^- under current and future facility operational configurations to meet groundwater treatment objectives after a planned expansion of the 200W P&T facility introduces additional groundwater contaminated with Tc-99 and U from beneath aging radioactive waste storage tanks. Physicochemical properties, including the nature of the

ligand, the hydration energy, and the size and charge of the anion, significantly affect the thermodynamics and kinetics of the exchange reactions with A532E. A532E is a bifunctional resin and has two quaternary ammonium functional groups with different sizes of alkyl chain length grafted onto the resin backbone. The long alkyl chain of the trihexylammonium group increases the hydrophobicity and enhances selectivity for TcO_4^-, whereas the triethylammonium group reduces steric congestion and facilitates faster uptake kinetics for poorly hydrated anions such as NO_3^- and TcO_4^- [28]. Based on the results of this work, the ability of A532E to remove TcO_4^- from solution is not significantly impacted by the presence of Cl^-, NO_3^-, SO_4^{2-}, and U over the concentration range tested, which represents the composition of current and future influent streams to the P&T. However, a slight increase in TcO_4^- in the final solution at very high NO_3^- loadings (≥ ~5 mM) may indicate that Tc removal (below 100%) could occur at high NO_3^- concentrations, but these concentrations are not representative of groundwater conditions. Because A532E is selective for poorly hydrated NO_3^-, HCO_3^- is displaced from the IX sites by NO_3^- at high NO_3^- concentrations. This suppresses the uptake of U as $UO_2(CO_3)_3^{4-}$, the dominant U species present under these conditions, as ligand exchange of CO_3^{2-} for NO_3^- is energetically unfavorable. Results demonstrate that U uptake by A532E decreases to as low as 38% in the presence of high concentrations of NO_3^-. This has implications for resin treatment train configuration as, unlike in the current configuration with DOWEX 21K resins for U removal in the first vessels (Figure S1), future designs for the IX system have A532E in the first vessels. The influence of NO_3^- concentration on U uptake by the A532E treatment train could result in a sudden increase in influent U concentration to the DOWEX 21K treatment train, which has the potential to impact IX resin performance.

Models informed by these batch sorption results predict equilibrium exchange coefficients for A532E uptake of NO_3^- ($K_{NO3-/Cl-} = 20$), SO_4^{2-} ($K_{SO42-/Cl-} = 0.2$), carbonate as HCO_3^- ($K_{HCO3-/Cl-} = 0.09$), Tc-99 as TcO_4^- ($K_{TcO4-/Cl-} = >4000$), and U as $UO_2(CO_3)_3^{4-}$ ($K_{U/Cl-} = 370 – 1000$). Given the sensitivity of anion interactions to variations in aqueous chemistry, especially in multicomponent systems, these equilibrium constants provide conservative parameters for predicting A532E performance for removal of Tc-99 from groundwater in the P&T facility. Based on these batch equilibrium constants, it is predicted that A532E will remove TcO_4^- from current and future influent streams such that effluent concentrations will meet groundwater treatment objectives, even in the presence of high concentrations of competing anions, NO_3^-, SO_4^{2-}, Cl^-, and HCO_3^-, and U(VI) carbonate as a co-contaminant. Future work will seek to confirm this prediction by optimizing the batch equilibrium IX constants to predict A532E performance under flow conditions. 1D column studies will be performed to further evaluate the degree to which kinetic effects, initially assessed here in batch experiments, affect A532E performance, with the batch-derived K values used in flow and transport modeling to fit Tc-99 breakthrough data. The model will ultimately be scaled up to predict IX performance as a function of changes in groundwater influent chemistry at the 200W P&T facility.

5 Acknowledgements

This document was prepared by the Deep Vadose Zone - Applied Field Research Initiative at

Pacific Northwest National Laboratory. Funding for this work was provided by the U.S. Department of Energy (DOE) Richland Operations Office. The Pacific Northwest National Laboratory is operated by Battelle Memorial Institute for the DOE under Contract DE-AC05-76RL01830.

6 Supporting Information

The following has been provided in the supporting information document: additional experimental procedure details, tabulated results from batch studies that support figures presented in the main text, schematic of the 200W P&T facility, contamination plume maps of the Hanford Central Plateau, GWB speciation plots, Tc and U plots from kinetic experiments, additional HYDROGEOCHEM modeling plots, and a comparison of A532E resin capacity for TcO_4^- to other material technologies.

References

[1] J.G. Speight, Natural Water Remediation Chemistry and Technology, Butterworth-Heinemann, 2020.
[2] J.W. Mercer, D.C. Skipp, D. Giffin, Basics of Pump-And-Treat Ground-Water Remediation Technology, Environmental Protection Agency (1990).
[3] I.M. Abrams, J.R. Millar, A history of the origin and development of macroporous ion-exchange resins, Reactive and Functional Polymers, 35 (1997) 7-22.
[4] C.D. Williams, P. Carbone, A classical force field for tetrahedral oxyanions developed using hydration properties: The examples of pertechnetate (TcO4−) and sulfate (SO42−), The Journal of Chemical Physics, 143 (2015) 174502.
[5] T.G. Levitskaia, E.L. Campbell, G.B. Hall, S. Chatterjee, D. Boglaienko, D.D. Reilly, M.A. Carlson, Characterization of spent Purolite A530E resin with implications for long-term radioactive contaminant removal, Journal of Environmental Chemical Engineering, 8 (2020) 104155.
[6] T.G. Levitskaia, E.L. Campbell, S. Chatterjee, G.B. Hall, Analysis of Technetium Ion Exchange Resin from the 200 West Pump-and-Treat Facility, PNNL-26933 United States 10.2172/1569474 PNNL English, ; Pacific Northwest National Lab. (PNNL), Richland, WA (United States) (2017).
[7] J.B. Duncan, Removal of Technetium 99 from the Effluent Treatment Facility (ETF) Basin 44 Using Purolite A-530E & Reillex HPQ & Sybron Ionac SR-7 Ion Exchange Resins, RPP-RPT-23199 Rev 0, Hanford Site (HNF) Richland, WA (United States) (2004).
[8] J.B. Duncan, K. Hagerty, W. Moore, J. Johnson, Laboratory Report on the Removal of Pertechnetate from Tank 241-AN-105 Simulant Using Purolite A530E, LAB-RPT-12-00002 Rev 0, Hanford Site Richland, WA (2012).
[9] B. Gu, Y.-K. Ku, G.M. Brown, Sorption and Desorption of Perchlorate and U(VI) by Strong-Base Anion-Exchange Resins, Environmental Science & Technology, 39 (2005) 901-907.
[10] M.M. Valenta, K.E. Parker, E.M. Pierce, Tc-99 Ion exchange resin testing, PNNL-19681, Pacific Northwest National Laboratory Richland, WA (United States) (2010).

[11] E.L. Campbell, T.G. Levitskaia, M.S. Fujimoto, V.E. Holfeltz, S. Chatterjee, G.B. Hall, Analysis of Uranium Ion Exchange Resin from the 200 West Pump-and-Treat Facility, PNNL-28062 United States 10.2172/1488863 PNNL English, ; Pacific Northwest National Lab. (PNNL), Richland, WA (United States) (2018).
[12] C. CH2M Hill Plateau Remediation Company, Draft Report – Technical Evaluation of Ion Exchange Vessels for the BP-5-PO1 System, CHPRC Richland, Washington (2020).
[13] Code of Federal Regulations, Maximum Contaminant Levels for Radionuclides, in: 40 CFR §141.66, 2020.
[14] DOE, 200-BP-5 and 200-PO-1 Groundwater Operable Units Feasibility Study for Interim Action, DOE/RL Richland, Washington (2018).
[15] P.D. Royer, T.P. Franklin, J.J. Garza, C.D. Johnson, N.J. Huerta, J.Q. Wassing, C.B. Woodford, J.P. Loftus, E.J. Engel, X. He, P.K. Tran, J.L. Fanning, V. Molina, F.J-V. Lopez, B.L. Armenta, A. Y.S., C.M.I. Brandao, T.L.N. Huynh, SOCRATES Software Release 2.0., PNNL-SA-167052, Pacific Northwest National Laboratory Richland, WA (2021).
[16] B. Gu, Y.-K. Ku, P.M. Jardine, Sorption and Binary Exchange of Nitrate, Sulfate, and Uranium on an Anion-Exchange Resin, Environmental Science & Technology, 38 (2004) 3184-3188.
[17] P.V. Bonnesen, G.M. Brown, S.D. Alexandratos, L.B. Bavoux, D.J. Presley, V. Patel, R. Ober, B.A. Moyer, Development of Bifunctional Anion-Exchange Resins with Improved Selectivity and Sorptive Kinetics for Pertechnetate: Batch-Equilibrium Experiments, Environmental Science & Technology, 34 (2000) 3761-3766.
[18] D. A.O., Langmuir, Freundlich, Temkin and DubiniŽ Radushkevich Isotherms Studies of Equilibrium Sorption of Zn 2+ Unto Phosphoric Acid Modified Rice Husk, IOSR Journal of Applied Chemistry, 3 (2012) 38-45.
[19] C. Bethke, S. Yeakel, The Geochemist's Workbench, in, Urbana, Illinois, 2009.
[20] R. Guillaumont, F.J. Mompean, Update on the chemical thermodynamics of uranium, neptunium, plutonium, americium and technetium, Elsevier Amsterdam, 2003.
[21] R.J. Lemire, Chemical thermodynamics of neptunium and plutonium, (2001).
[22] I. Grenthe, X. Gaona, A. Pyasunov, L. Rao, W. Runde, B. Grambow, R.J.M. Konings, A.L. Smith, E.E. Moore, Second Update on the Chemical Thermodynamics of Uranium, Neptunium, Plutonium, Americium and Technetium, OECD, Paris, France, 2020.
[23] G.-T. Yeh, Y. Fang, F. Zhang, J. Sun, Y. Li, M.-H. Li, M.D. Siegel, Numerical modeling of coupled fluid flow and thermal and reactive biogeochemical transport in porous and fractured media, Computational Geosciences, 14 (2010) 149-170.
[24] Y. Fang, S.B. Yabusaki, G.-T. Yeh, A general simulator for reaction-based biogeochemical processes, Computers & geosciences, 32 (2006) 64-72.
[25] Y. Fang, G.T. Yeh, W.D. Burgos, A general paradigm to model reaction-based biogeochemical processes in batch systems, Water Resources Research, 39 (2003).
[26] J. Li, L. Zhu, C. Xiao, L. Chen, Z. Chai, S. Wang, Efficient uptake of perrhenate/pertechnenate from aqueous solutions by the bifunctional anion-exchange resin, Radiochimica Acta, 106 (2018) 581-591.
[27] W.A. de Jong, E. Aprà, T.L. Windus, J.A. Nichols, R.J. Harrison, K.E. Gutowski, D.A. Dixon, Complexation of the Carbonate, Nitrate, and Acetate Anions with the Uranyl Dication: Density Functional Studies with Relativistic Effective Core Potentials, The Journal of Physical Chemistry A, 109 (2005) 11568-11577.

[28] P.A. Mosier-Boss, Use of Raman spectroscopy to evaluate the selectivity of bifunctional anion exchange resins for perchlorate, Appl Spectrosc, 62 (2008) 157-165.
[29] P.D. Royer, T.P. Franklin, J.J. Garza, C.D. Johnson, N.J. Huerta, J.Q. Wassing, e.a. C.B. Woodford, SOCRATES software release 2.0, Pacific Northwest National Laboratory, Richland, WA., PNNL-SA-167052 (2021).

Table 1. Composition of Tc-99 ion exchange (IX) influent stream, Tank Y20 [29].

Parameter/Type	Units	Average	Std. Dev.	Number of Measurements
From 6/1/2020 through 5/30/2021		**Y20 (Tc-99 influent)**		
Technetium-99	**pCi/L**	**1350**	**380**	**11**
Uranium	**µg/L**	**1.25**	**0.18**	**22**
Nitrate	µg/L	115,000	10,000	12
Sulfate	µg/L	65,000	11,000	12
Chloride	µg/L	19,400	3,700	12
From 6/1/2021 through 5/30/2022		**Y20 (Tc-99 influent)**		
Technetium-99	**pCi/L**	**1230**	**140**	**12**
Uranium	**µg/L**	**1.71**	**0.37**	**24**
Nitrate	µg/L	100,000	4,000	12
Sulfate	µg/L	57,200	8,800	12
Chloride	µg/L	18,200	2,200	12

653 **Table 2**. Experiment matrix with target Cl^-, CO_3^{2-}, NO_3^-, SO_4^{2-}, Tc and U concentrations used in Cl^- treated A532E resin batch
654 sorption experiments. The starting solution pH before A532E addition was 7.4 ± 0.1.

Test	Solution:Solid Ratio (mL/g dry resin)*	Cl^- mM (ppm)&	CO_3^{2-} mM (ppm)	NO_3^- or SO_4^{2-} mM (ppm)%,$	Tc-99 (ppb)	U (ppb)	Test Objective
A	52 – 1044	13 (459)**	10 (600)	-	-	-	Quantify only CO_3^{2-} uptake
NO_3^- Experiments							
B	50 - 992	-	-	3.3 (203)	-	-	Quantify only NO_3^- uptake
C	201 – 203	0.06 – 205 (2 - 7072)	-	3.2 – 3.4 (199 – 211)	-	-	Evaluate NO_3^- uptake as a function of $[Cl^-]$
D	51 - 1015	57 – 73 (2030 – 2600)	-	3.0 (185)	-	-	Quantify NO_3^- uptake in the presence of optimal $[Cl^-]$
E	51 - 1006		10 (600)	3.0 (187)	-	-	Quantify NO_3^- and CO_3^{2-} uptake in the presence of optimal $[Cl^-]$
F	199 – 201		-	<0.02 – 20.3 (<1.32 – 1260)	200	-	Determine the effect of $[NO_3^-]$ on Tc-99 uptake in the presence of optimal $[Cl^-]$
G	200		10 (600)	<0.02 – 19.5 (<1.32 – 1210)	-	116	Determine the effect of $[NO_3^-]$ on U uptake in the presence of 10 mM CO_3^{2-} and optimal $[Cl^-]$
H	208 – 209		10 (600)	<0.02 – 18.7 (<1.32 – 1160)	200	116	Determine the effect of $[NO_3^-]$ on U and Tc-99 uptake in the presence of 10 mM CO_3^{2-} and optimal $[Cl^-]$
S	197 - 201		10 (600)	<0.04 – 18.7 (<2.3 – 1160)	200	-	Determine the effect of $[NO_3^-]$ on Tc-99 uptake in the presence of 10 mM CO_3^{2-} and optimal $[Cl^-]$
SO_4^{2-} Experiments							
I	49 – 957	0.04 (1.5)	-	3.0 (292)	-	-	Quantify only SO_4^{2-} uptake
J	200 – 202	1 – 211 (39 – 7490)	-	2.9 – 3.1 (277 – 298)	-	-	Evaluate SO_4^{2-} uptake as a function of $[Cl^-]$
K	51 -1002	65 (2310)	10 (600)	3.1 (293)	-	-	Quantify SO_4^{2-} uptake in the presence of 10 mM CO_3^{2-} and optimal $[Cl^-]$
L	201 – 203	51 – 52 (1810 – 1830)	-	<0.05 – 10.0 (<5.05 – 958)	200	-	Determine the effect of $[SO_4^{2-}]$ on Tc-99 uptake in the presence of optimal $[Cl^-]$
M	201 – 202	54 – 56 (1910 – 1980)	10 (600)	<0.05 – 10.4 (<5.05 – 1000)	-	116	Determine the effect of $[SO_4^{2-}]$ on U uptake in the presence of 10 mM CO_3^{2-} and optimal $[Cl^-]$
N	201 - 202	51 – 52 (1800 - 1830)	10 (600)	<0.05 – 9.9 (<5.05 – 951)	200	116	Determine the effect of $[SO_4^{2-}]$ on U and Tc-99 uptake in the presence of 10 mM CO_3^{2-} and optimal $[Cl^-]$
Q	51 - 997	53 (1880)	-	3.1 (297)	-	-	Quantify SO_4^{2-} uptake in the presence of optimal $[Cl^-]$

Test	Solution:Solid Ratio (mL/g dry resin)[*]	Cl^- mM (ppm)[&]	CO_3^{2-} mM (ppm)	NO_3^- or SO_4^{2-} mM (ppm)[%,$]	Tc-99 (ppb)	U (ppb)	Test Objective
R	201 – 202	61 – 63 (2160 – 2240)	10 (600)	<0.05 – 9.8 (<5.05 – 940)	200	-	Determine the effect of [SO_4^{2-}] on Tc-99 uptake in the presence of 10 mM CO_3^{2-} and optimal [Cl^-]
Test	**Solution:Solid Ratio (mL/g dry resin)[*]**	**Cl^- mM (ppm)[&]**	**CO_3^{2-} mM (ppm)**	**NO_3^- or SO_4^{2-} mM (ppm)[%,$]**	**Tc-99 (ppb)**	**U (ppb)**	**Test Objective**
Kinetic Experiments							
T	1000	50 (1768)	10 (600)	19 (1190) for NO_3^- and 5 (500) for SO_4^{2-}	200	116	Determine the kinetics of U and Tc uptake in the presence of all anions

Legend:

[*]Ratio [**50 – 1000**]: 50, 100, 200, 500, and 1000 mL/g dry resin

[&]Cl^- [**0 to 200 (7072**)]: 0, 10 (354), 50 (1768), 100 (3536), and 200 (7072) mmol/L (ppm)

[%]NO_3^- [**0 to 19 (1190**)]: 0, 1.5 (95), 3 (190), 5 (313), 10 (625), and 19 (1190) mmol/L (ppm)

[$]$SO_4^{2-}$ [**0 to 10 (1000**)]: 0, 0.5 (50), 2 (150), 5 (500), and 10 (1000) mmol/L (ppm)

[**] Presence of Cl^- due to pH adjustment.

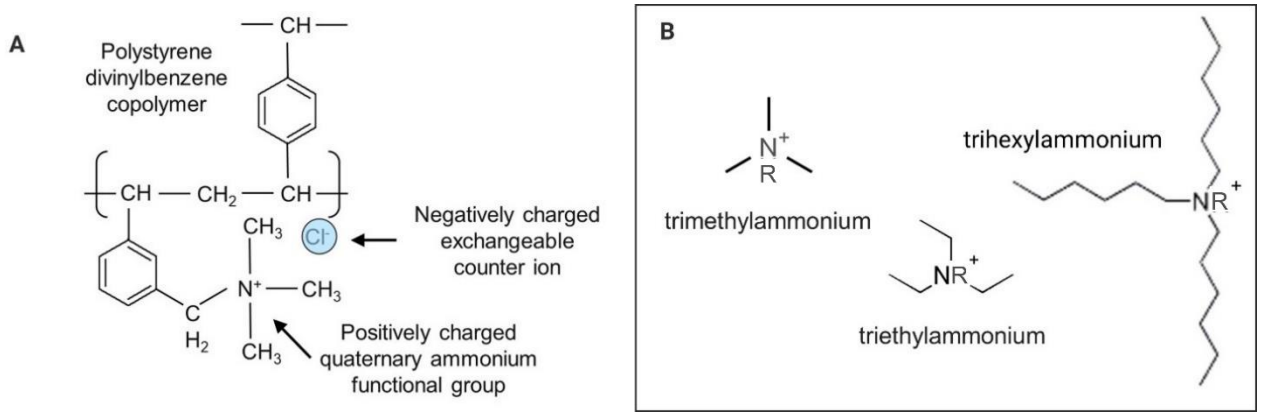

Figure 1. **(A) Chemical form of a Type I strong base anion exchange resin.** (B) Typical quaternary amine exchange sites found on strong base anion exchange resins; **Purolite A532E** has bifunctional **triethylammonium and trihexylammonium** exchange sites, and DOWEX 21K has **trimethyl ammonium** exchange sites.

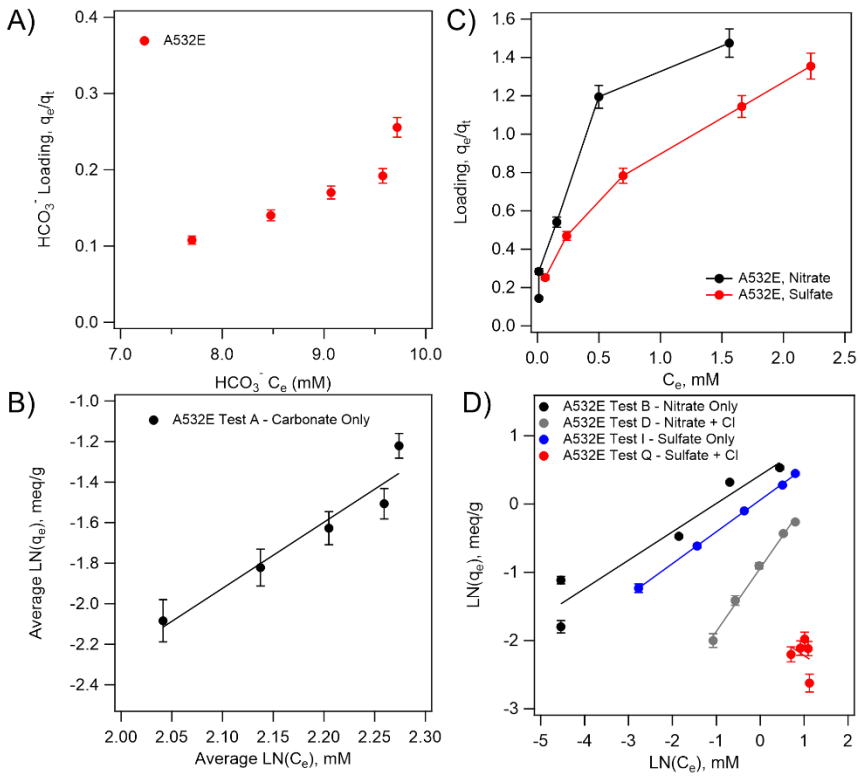

Figure 2. Sorption isotherms with HCO_3^- (A) and Freundlich fit with HCO_3^- (B). Sorption isotherms with NO_3^- and SO_4^{2-} (C), and Freundlich fit with or without Cl^- in addition with NO_3^- and SO_4^{2-} (D). In A and C, uptake by A532E resins is presented as a fractional loading q_e/q_t of the target anion, where q_e is the equilibrium loading for this anion and q_t is the total ion-exchange capacity of the resin (q_t = 1.12 meq/g dry resin). Initial concentrations of CO_3^{2-}, NO_3^-, or SO_4^{2-} in solution were 10 mM, 3 mM, or 3 mM, respectively. The solution-to-resin phase ratio varied from 50 – 1000 mL/g dry resin on the dry resin basis. Testing was conducted at ambient temperature. Error bars indicate the experimental error of ± 5%.

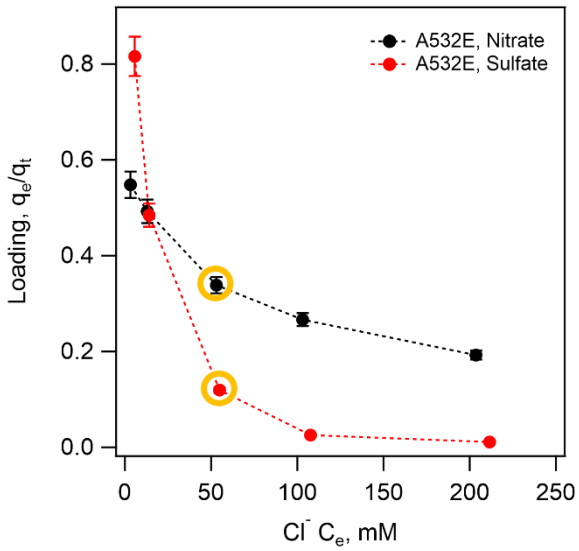

671

672 **Figure 3.** Sorption isotherms for NO_3^- and SO_4^{2-} uptake at different Cl^- concentrations for
673 A532E resins, presented as a fractional loading q_e/q_t of the target anion, where q_e is the
674 equilibrium loading for this anion and q_t is the total ion-exchange capacity of the resin (q_t = 1.12
675 meq/g dry resin). Cl^- concentrations ranged from 0 – 200 mM. Testing was conducted at ambient
676 temperature. The optimal Cl^- concentration point chosen, 50 mM, is identified by a gold open
677 circle. Error bars indicate the experimental error of ± 5%.

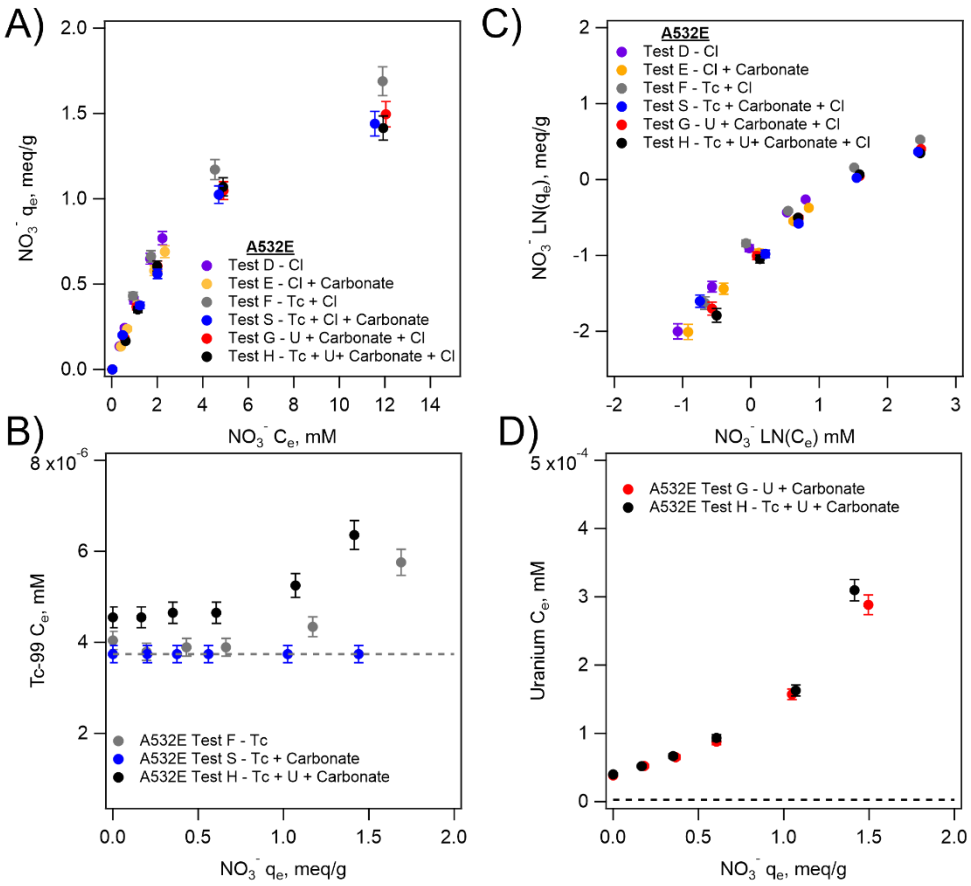

678

679 **Figure 4.** A532E NO_3^- sorption (A) and Freundlich (C) isotherms for all experiments containing
680 NO_3^- except Tests B and C. The effect of NO_3^- loading on the final aqueous concentrations of Tc-
681 99 and U is shown in panels (B) and (D), respectively. The small y-axis range in (B) shows the
682 increase in Tc-99 C_e values, but note that these values are within rounding to 100% uptake. The
683 dashed lines indicate the ICP-MS limit of detection for Tc-99 (3.74×10^{-6} mM) and for U ($2.55 \times$
684 10^{-6} mM). Error bars indicate the experimental error of ± 5%.

685

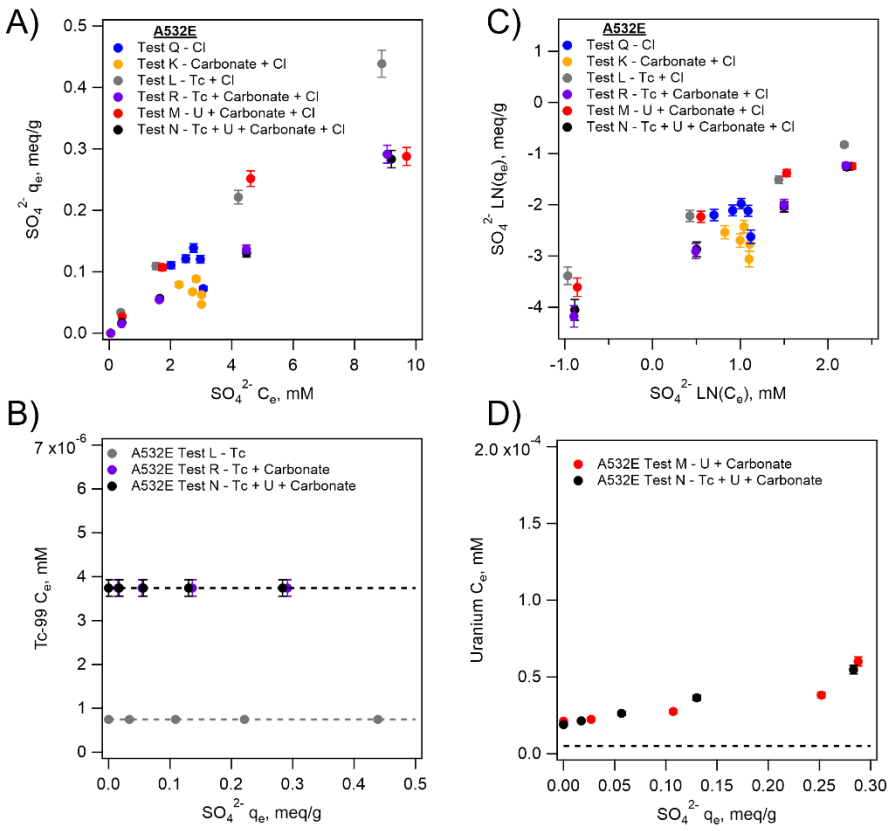

686

687 **Figure 5.** A532E SO_4^{2-} sorption (A) and Freundlich (C) isotherms for all experiments containing
688 SO_4^{2-} except Tests I and J. The effect of SO_4^{2-} loading on the final aqueous concentrations of Tc-
689 99 and U is shown in panels (B) and (D), respectively. The dashed lines indicate the ICP-MS limit
690 of detection for Tc-99 (3.74×10^{-6} mM, black line Tests R and N; 7.48×10^{-7} mM, grey line, Test
691 L) and for U (5.10×10^{-6} mM). The Tc-99 solution concentration could not be determined because
692 it was below the ICP-MS limit of detection for Tc-99. Error bars indicate the experimental error
693 of ± 5%.

694

695

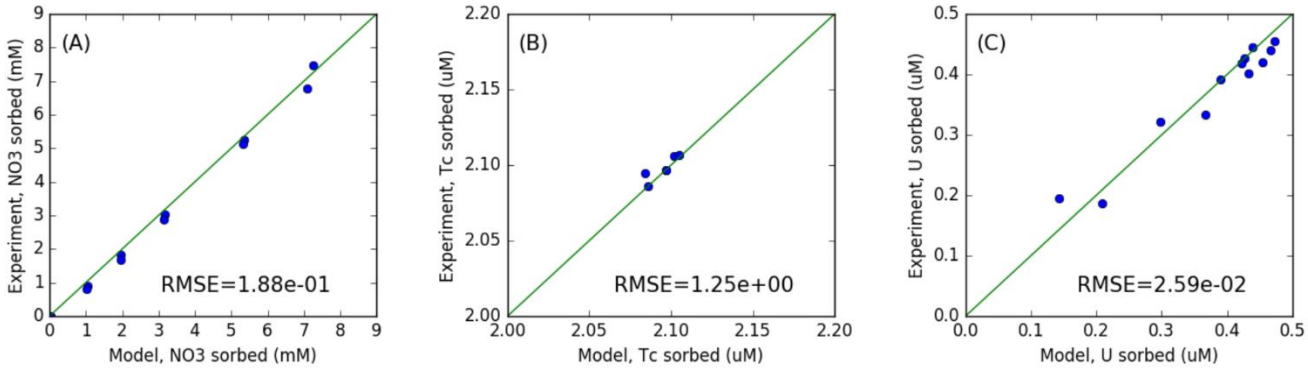

696

697 **Figure 6.** Comparison between the measured values and model results for (A) NO_3^-, (B) Tc-99,
698 and (C) U in A532E Test G and Test H. Reported values for $K_{NO3-/Cl-}$ (20), $K_{TcO4-/Cl-}$ (>4000), and
699 $K_{U/Cl-}$ (500) represent the K values where the root mean square error (RMSE) value was
700 minimized for the specific anion and dataset used for fitting.